

Toward the Design of Photoresponsive Conditional Antivitamins B₁₂: A Transient Absorption Study of an Arylcobalamin and an Alkynylcobalamin

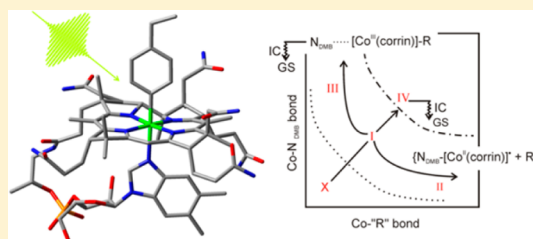
Nicholas A. Miller,[†] Theodore E. Wiley,[†] Kenneth G. Spears,[†] Markus Ruetz,[‡] Christoph Kieninger,[‡] Bernhard Kräutler,[‡] and Roseanne J. Sension^{*,†}

[†]Department of Chemistry, University of Michigan, Ann Arbor, Michigan 48109-1055, United States

[‡]Institute of Organic Chemistry & Center for Molecular Biosciences, University of Innsbruck, Innrain 80/82, A-6020 Innsbruck, Austria

Supporting Information

ABSTRACT: Cobalamins are of widespread importance in biology. Both of the cofactors essential for human metabolism, the organocobalamins coenzyme B₁₂ and methylcobalamin, are highly photolabile, as are other alkylcobalamins. The alkynylcobalamin phenylethynylcobalamin (PhEtyCbl) and the arylcobalamin 4-ethylphenylcobalamin (EtPhCbl) with “atypical” Co–C-bonds to unsaturated carbons, were recently designed as metabolically inert cobalamins, classified as “antivitamins B₁₂”. The further development of an ideal light-activated or “conditional” antivitamin B₁₂ would require it to be readily converted by light into an active B₁₂ vitamin form. Very photolabile “antivitamins B₁₂” would also represent particularly useful scaffolds for therapeutic light-activated reagents. Here, the photoactive arylcobalamin EtPhCbl and the remarkably photostable alkynylcobalamin PhEtyCbl are examined using femtosecond to picosecond UV–visible transient absorption spectroscopy. PhEtyCbl undergoes internal conversion to the ground state with near unit quantum yield on a time scale < 100 ps and an activation energy of 12.6 ± 1.4 kJ/mol. The arylcobalamin EtPhCbl forms an excited state with a ca. 247 ps lifetime. This excited state branches between internal conversion to the ground state and formation of a long-lived base-off species with a quantum yield of ~9%. Anaerobic steady state photolysis of “light-sensitive” EtPhCbl results in the formation of cob(II)alamin, but only with quantum yield <1%. Hence, our studies suggest that suitably modified arylcobalamins may be a rational basis for the design of photoresponsive “antivitamins B₁₂”.



INTRODUCTION

Cobalamins such as vitamin B₁₂ (Figure 1) are essential human nutrients providing the cofactors adenosylcobalamin (AdoCbl) for methylmalonyl CoA mutase and methylcobalamin (MeCbl) for methionine synthase.^{1,2} These cobalamin-dependent enzymes and a range of additional B₁₂-dependent radical

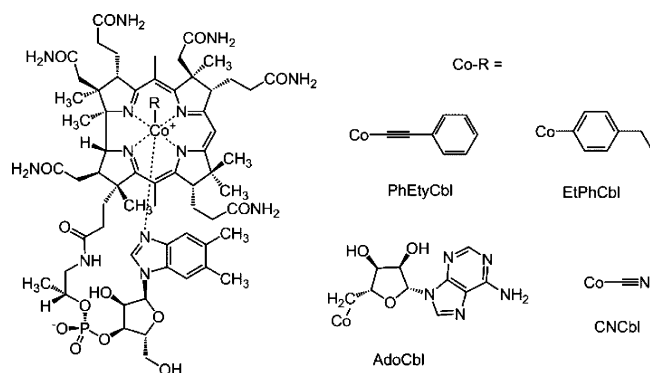


Figure 1. Vitamin B₁₂ (CNCbl) and organometallic analogues.

isomerases and methyl transferases are found in other organisms, especially bacteria.^{3–5} The consequences of vitamin B₁₂ deficiency for human health are severe and a subject of intense ongoing investigation.^{6,7} Antivitamins B₁₂ are a new class of cobalamins designed to mimic B₁₂ deficiency and enable the study of the health consequences in animal models under controlled conditions.⁸ The ideal “antivitamin B₁₂” is a metabolically inert cobalamin taken up by the B₁₂ transport proteins and resistant to the enzyme CblC⁸ that “tailors” vitamin B₁₂ (cyanocobalamin, CNCbl) and other cob(III)-alamins for the purpose of their intracellular conversion into a biologically active form.^{9,10}

Organometallic arylcobalamins are a novel class of B₁₂-derivatives,¹¹ and alkynylcobalamins were, likewise, scarcely known and hardly characterized until recently.^{12–14} Both types of organocobalamins have recently become available and crystalline pure samples of two of them were further analyzed here: 4-ethylphenylcobalamin (EtPhCbl)¹¹ and phenylethynylcobalamin (PhEtyCbl).^{12,14} EtPhCbl has been shown to impair

Received: May 23, 2016

Published: October 24, 2016

tissue uptake and cause functional B₁₂ deficiency in laboratory mice,¹⁵ and has, thus, been classified as an “antivitamin B₁₂”.⁸ Both, EtPhCbl and PhEtyCbl, are thermally stable and resistant to reduction to cob(II)alamin. PhEtyCbl is photostable, but illumination with diffuse day light in the presence of oxygen causes EtPhCbl to undergo photolysis to form aquocobalamin (H₂Ocbl).¹¹ It has been suggested that EtPhCbl or similar arylcobalamins represent “conditional antivitamin B₁₂”,⁸ which, by using excitation with visible light, may be “unlocked” and, thus, induced to uncage their hidden B₁₂-vitamin function in a controlled fashion.

The two important B₁₂-cofactors, coenzyme B₁₂ and methylcobalamin, and other alkylcobalamins have, so far, been found to be characteristically photolabile.^{16,17} Hence, the photoactivity of cobalamins has been the focus of a number of recent experimental¹⁷ and theoretical investigations.¹⁸ The discovery of a bacterial protein, CarH, that exploits AdoCbl photolysis for light-activated gene regulation^{19–23} and increasing research into cobalamins as light-activated agents for controlled spatiotemporal delivery of therapeutic agents provide additional motivation for these studies.^{24–26} Photolabile and metabolically inert cobalamins, i.e., photoactive “antivitamins B₁₂” could represent particularly useful scaffolds for therapeutic light-activated reagents. Thus, the apparently divergent photochemistry of EtPhCbl and PhEtyCbl presents an interesting challenge. What factors control the photochemistry of their Co–C bonds to unsaturated carbons?

Here we report time-resolved spectroscopic studies of the arylcobalamin EtPhCbl and the alkynylcobalamin PhEtyCbl, two potential “antivitamins B₁₂”, and discuss the results in the context of experimental and theoretical studies of a range of cobalamin derivatives. Neither of these two organocobalamins with “atypical” Co–C bonds undergoes prompt bond homolysis with measurable yield. PhEtyCbl undergoes internal conversion to the ground state with essentially unit quantum yield on a time scale < 100 ps. EtPhCbl forms an excited state with a ca. 247 ps lifetime. This excited state branches between internal conversion to the ground state and formation of a long-lived base-off species where the lower axial 5,6-dimethylbenzimidazole (DMB) ligand is decoordinated. This base-off species is formed with a quantum yield of ~9% and a lifetime much longer than the 4 ns limit of our transient absorption measurements. Anaerobic photolysis of EtPhCbl in the visible or near UV regions of the spectrum results in the formation of cob(II)alamin, but the quantum yield is <1%, consistent with the transient absorption measurements.

EXPERIMENTAL METHODS

Femtosecond transient absorption measurements were performed using a Ti:sapphire laser system operating at a 1 kHz repetition rate. A pump wavelength of 400 nm was generated as the second harmonic of the laser system. A pump wavelength of 550 nm was generated using a home-built noncollinear optical parametric amplifier pumped by the Ti:sapphire laser. Broadband probe pulses were generated by focusing either the fundamental or second harmonic of the laser into a 3 mm translating CaF₂ window. The resulting continua together span the wavelength region from 290 to 700 nm. Measurements were obtained by overlapping the pump and probe focus in a 1 mm quartz cell, with the relative polarization directions at magic angle. A 1 mm flow cell was used for 400 nm pump measurements on EtPhCbl. Samples of EtPhCbl and PhEtyCbl were prepared by dissolving 2 mg of the pure crystalline compounds synthesized and purified as described earlier^{11,12} in 2 mL deionized water resulting in a nominal concentration of 0.7 mM. Analysis of the transient spectra was carried out using the

freely available global analysis program Glotaran²⁷ or a more flexible Python-based program VarPro developed in our laboratory.²⁸

UV–vis spectra were collected on a Shimadzu UV-2600 spectrometer. UV–visible spectra are shown in Figure 2. PhEtyCbl

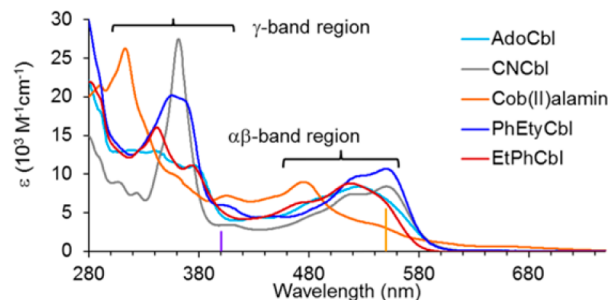


Figure 2. UV–visible spectra comparing several cob(III)alamins with the two antivitamin B₁₂ compounds studied here. The excitation wavelengths used for transient absorption measurements are indicated by the vertical lines at 400 nm (violet) and 550 nm (yellow).

has a structured $\alpha\beta$ -band absorption similar to CNCbl and a well-defined γ -band.¹² EtPhCbl has a blue-shifted $\alpha\beta$ -band more similar to AdoCbl and two separated γ -band peaks.¹¹

Steady-state photolysis measurements were performed using a sample prepared by dissolving the compound and an excess of radical scavenger (TEMPO) in deoxygenated water. The ultraviolet and visible continua were generated with a xenon arc lamp and various filter combinations. PhEtyCbl is photostable under the conditions of our measurements (quantum yield $\phi < 10^{-5}$) while EtPhCbl exhibits slow photolysis with UV excitation or visible excitation ($\phi < 0.01$). See Supporting Information Figures S1–S4.

RESULTS

Phenylethynylcobalamin. Alkynyl-cobalamins have been reported to be remarkably light-stable,¹² contrasting with the situation of typical organocobalamins.^{17,29,30} Here the primary photochemistry of an alkynylcobalamin, PhEtyCbl, on the femtosecond and picosecond time scale is investigated using 400 nm excitation and 550 nm excitation (see Figure 2) for temperatures near 20 °C. Similar results are obtained at both excitation wavelengths. The data obtained with 400 nm excitation is summarized in Figure 3.

The data were fit to a model consisting of a sum of exponential decay components. Following excitation at 400 nm there is evidence for a fast component < 100 fs. A fast internal conversion component may be expected when exciting with energies well above the lowest excited state, but analysis of this

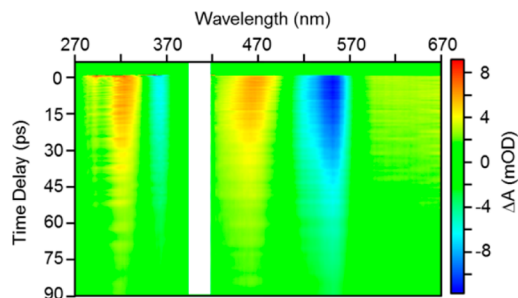


Figure 3. Transient absorption measurement following excitation of PhEtyCbl at 400 nm. This is a composite from measurements performed using continuum generated with 400 nm (270–600 nm) and 800 nm (370–770 nm) pulses.

component in the data is complicated by coherent signals including two-photon absorption, stimulated Raman and cross-phase modulation from the sample, solvent, and cell wall. On a longer time-scale three components are obtained: $\tau_A = 0.53$ ps, $\tau_B = 8.5$ ps, and $\tau_C = 62$ ps. Transient signals and fits at four characteristic wavelengths illustrating the necessity for these three decay components are plotted in Figure 4. The fastest

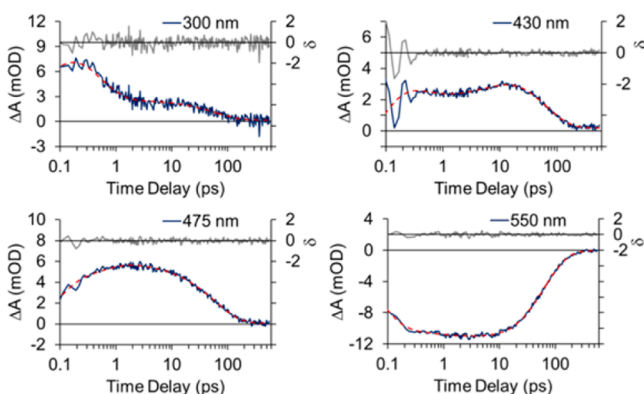


Figure 4. Transient signals at four characteristic wavelengths plotted on a logarithmic time scale (blue lines). The fits (red dashed lines) and residuals (gray lines) are also plotted.

component $\tau_A = 0.53$ ps is prominent at 300 and 475 nm. The intermediate component $\tau_B = 8.5$ ps is most obvious at 430 nm. The decay of the excited state on a 62 ps time scale is apparent at all probe wavelengths. The same three components are observed following excitation directly into the lowest vertical excited state at 550 nm: $\tau_A = 0.53$ ps, $\tau_B = 8.6$ ps, and $\tau_C = 56$ ps. Again, there may be a faster component reflecting internal conversion from the optically allowed state populated by the excitation pulse, but it is overlapped with coherent signals that complicate the interpretation. The variation in τ_C is attributed to small changes in the room temperature (see below).

The decay associated difference spectra (DADS) representing the amplitudes as a function of wavelength for each decay component are plotted in Figure 5a. There is no significant dependence on excitation wavelength for time delays longer than a few hundred femtoseconds.

Assuming a sequential model, Ground State (GS) $\xrightarrow{h\nu}$ A $\xrightarrow{\tau_A}$ B $\xrightarrow{\tau_B}$ C $\xrightarrow{\tau_C}$ GS, the decay associated spectra (DADS) can be used to estimate species associated difference spectra (SADS). A derivation of the appropriate formulas is provided in the Supporting Information. The SADS plotted in Figure 5b are characterized by a diffuse absorption extending deep into the red, a decrease in absorption in the region of the $\alpha\beta$ - and γ -bands and an increase of absorption to the blue of each band characteristic of blue-shift of these transitions in the excited state.

The SADS can be used to estimate the excited state spectra by adding the appropriately scaled ground state spectrum to the difference spectra: $I_x(\lambda) = \Delta A_x(\lambda) + \alpha I_{GS}(\lambda)$, where ΔA_x is the SADS for intermediates $x = A, B,$ or C and α is the percent of ground state excited determined by the intensity of the excitation pulse and the absorbance of the sample. The best estimate for the data reported in Figure 5 is $\alpha = 2$ –2.5%. The excited state spectra allow more insight into the nature of the lowest singlet excited state S_1 responsible for the photochemistry or photostability of cobalamins. The intermediates

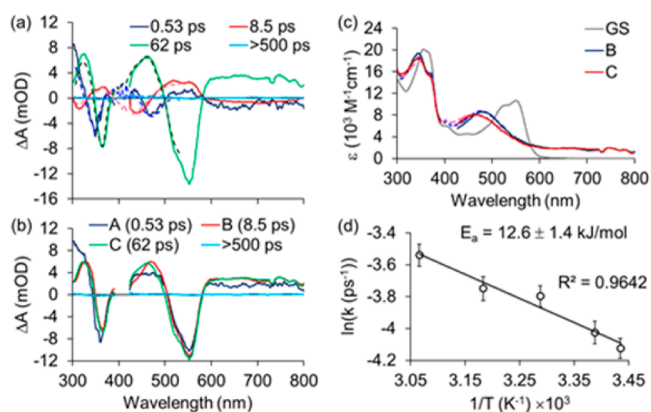


Figure 5. (a) Decay associated difference spectra (DADS) associated with the exponential decay components. Solid lines represent the results obtained following excitation at 400 nm, and dashed lines are the more limited spectral range measured after excitation at 550 nm. Wavelength scale is below (b). (b) Species associated difference spectra (SADS) obtained following excitation at 400 nm. (c) Estimated spectra for states B and C obtained by adding the ground state spectrum (GS) to the respective SADS. (d) Arrhenius plot for the ground state recovery following excitation of PhEtCbl in aqueous solution.

designated B and C have similar spectra, characterized by a blue-shifted $\alpha\beta$ -band and change in the structure of the γ -band. The similarity in these spectra suggests that the transition from B to C may involve a modest conformational change on the excited state surface. Comparison with other cobalamins leads to the hypothesis that the axial bonds in the excited electronic state are elongated from the ground state structure.^{31,32}

The internal conversion of the S_1 state “C” to the ground state is a barrier crossing process. The decay constant was determined over a temperature range from 18 °C ($\tau_C = 62$ ps) to 53 °C ($\tau_C = 34$ ps). Assuming Arrhenius behavior with both the activation energy (E_a) and prefactor (A_h) independent of temperature, we have $\ln k = -\frac{E_a}{R} \frac{1}{T} + \ln A_h$ and the observed rate constants can be used to estimate the activation barrier for internal conversion to the ground state. The result is presented in Figure 5d. The temperature dependence of the faster decay components is not reported as the decays are difficult to extract with precision from the data and have no clear trend related to barrier crossing processes. The barrier for internal conversion to the ground state of 12.6 ± 1.4 kJ/mol is higher than that estimated for CNCbl in aqueous solution (8.8 ± 0.8 kJ/mol), but similar to the extrapolated gas phase value for CNCbl (12.5 ± 0.5 kJ/mol) and consistent with a similar mechanism for internal conversion to the ground state.^{31,33}

4-Ethylphenylcobalamin. Steady-state photolysis measurements on EtPhCbl using visible or near UV light exhibits slow photolysis forming cob(II)alamin (and a radical). Exposure of aerated solutions of EtPhCbl to day light resulted in decomposition to aquocobalamin.¹¹ However, comparison of the rate of photolysis with cobalamins that undergo rapid photolysis with high quantum yield suggests that the quantum yield for photolysis of EtPhCbl is <1%. See the Supporting Information for details and plots of the steady state photolysis measurements.

Transient absorption measurements on EtPhCbl were performed using 400 nm excitation and 550 nm excitation for temperatures near 20 °C. The spectral evolution following 400

nm excitation is summarized in Figure 6. As with PhEtCbl, similar results are obtained at both excitation wavelengths.

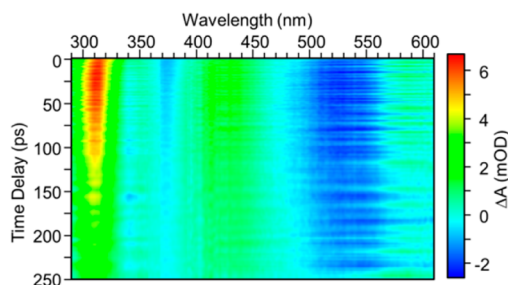


Figure 6. Transient absorption data obtained following excitation of EtPhCbl at 400 nm.

The data was fit to a model consisting of a sum of exponential decay components. There is evidence for evolution corresponding to rapid internal conversion < 200 fs, but analysis of this component is complicated by coherent signals including two-photon absorption, stimulated Raman and cross-phase modulation from the sample, solvent, and cell wall. On a longer time-scale four components are obtained following excitation at 550 nm: $\tau_A = 0.57$ ps, $\tau_B = 13.4$ ps, and $\tau_C = 247$ ps and a long-lived product with $\tau_D \gg 4$ ns. Following 400 nm excitation the earliest component is not well-defined, but on longer time scales the time constants are consistent with those observed following 550 nm excitation: $\tau_B = 13.0$ ps, and $\tau_C = 240$ ps.

Transient signals and fits at several characteristic wavelengths illustrating the necessity for these three decay components are plotted in Figure 7. The fastest component $\tau_A = 0.57$ ps is prominent at 312 nm. The intermediate component $\tau_B = 13.4$ ps is most obvious at 312 and 529 nm.

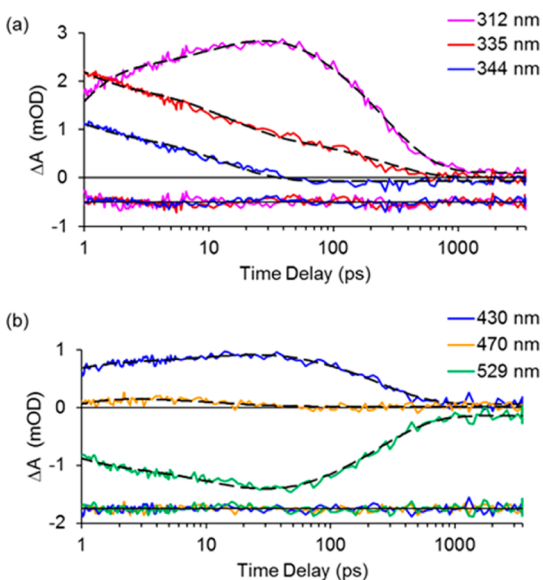


Figure 7. (a) Kinetic traces at three characteristic UV wavelengths following excitation of EtPhCbl at 550 nm. Dashed lines represent fits to the data as described in the text. The residuals (data-fit) are plotted on the same scale, offset by -0.5 for clarity. (b) Kinetic traces at three characteristic visible wavelengths. Residuals are offset by -1.75 for clarity.

Assuming a sequential model, the SADS corresponding to the longer two decay components are plotted in Figure 8a. The

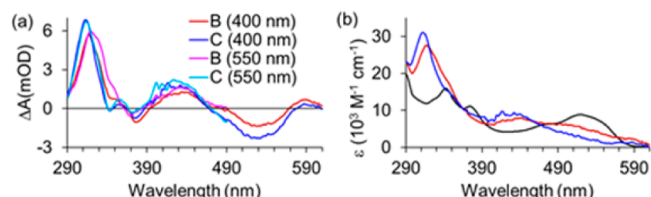


Figure 8. (a) SADS obtained from the fits to the transient absorption data. Excitation wavelengths are indicated. (b) Excited state spectra estimated by adding the ground state spectrum of EtPhCbl to the SADS obtained with 400 nm excitation (red B, blue C). Black line is the ground state spectrum of EtPhCbl.

spectrum corresponding to B is slightly different for the two excitation wavelengths between 320 and 350 nm, but the spectrum of C is independent of excitation wavelength. The estimated excited state spectra determined by adding the ground state spectrum back into the difference spectra are plotted in Figure 8 b. Again the excitation percentage was $\sim 2\%$. The relaxed excited state spectrum of C exhibits a prominent γ -band at 312 nm and a blue-shifted $\alpha\beta$ -band peaking near 430 nm. The position of the $\alpha\beta$ -band is characteristic of an elongated bond or dissociated lower axial ligand, although the γ -band position and intensity is more consistent with formation of cob(II)alamin. In composite, the excited state spectrum is consistent with elongation of bonds to both the upper and lower axial ligands.

The long-lived product persisting for delay times $\gg 4$ ns is consistent with formation of base-off EtPhCbl. The base-off–base-on difference spectrum is compared with the observed transient difference spectrum in Figure 9. The spectral shape is

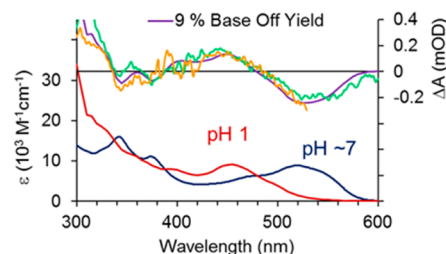


Figure 9. Comparison of the difference spectrum (purple) between base-on (blue, pH 7) and base-off (red, pH 1) EtPhCbl with the long-lived photoproduct observed in the transient absorption measurements (yellow 550 nm excitation, green 400 nm excitation). The base-off–base-on difference spectrum is scaled to the nanosecond difference spectra, resulting in an estimated 9% yield of the base-off product.

nearly identical and the magnitude of the long-lived signal is consistent with a quantum yield of ca. 9% formation of the base-off product. There is no evidence for formation of cob(II)alamin above the noise-level of the data. The measurements are insensitive to quantum yields of bond homolysis $< 1\%$.

DISCUSSION

Typical organo-cobalamins, such as coenzyme B_{12} (AdoCbl) and methylcobalamin (MeCbl), are notoriously photolabile, requiring protection from light in experiments with these two B_{12} -cofactors.¹⁷ However, photolability may also be essential for

their biological function, as was recently recognized in studies of a widespread form of bacterial B₁₂-dependent photo-regulation, which is based on the photocleavage of the Co–C-bond of protein-bound AdoCbl.^{21,23,34} Arylcobalamins and alkynylcobalamins were recently prepared by us and proposed to be metabolically inert, potential antivitamin B₁₂, as a consequence of the nature of their atypical organometallic bond involving unsaturated, cobalt-bound C.^{11,12} These novel types of antivitamin B₁₂ induce 'functional' B₁₂ deficiency in laboratory animals,¹³ a condition that may help decipher still elusive physiological roles of vitamin B₁₂ and other natural cobalamins in mammals. Furthermore, suitably designed antivitamin B₁₂ are a novel group of potential antibiotics and anticancerous agents.⁸ The atypical Co–C-bonds of aryl- and alkynyl-cobalamins are key elements in stabilizing these B₁₂-derivatives against metabolic transformation by cleavage of their organometallic bonds. Their Co–C-bonds also influence the photochemical cleavage, limiting (in the aryl-cobalamin EtPhCbl) or eliminating (in the alkynyl-cobalamin PhEtyCbl) photoinduced bond homolysis. We report here the first detailed photochemical studies of B₁₂ derivatives with such an unsaturated organic carbon bonded to the cobalt. Further analysis of these results in the context of other cobalamins and theoretical simulations will shed light on the parameters required for photostability or facile bond cleavage of organo-cobalamins.

Kozłowski and co-workers have reported extensive DFT and TD-DFT calculations on several species including models for CNCbl, hydroxocobalamin (HOCbl), AdoCbl, and MeCbl, along with more limited calculations on ethylcobalamin (EtCbl).^{18,33,35–41} These calculations of the electronic excited states highlight the influence of a seam between a metal-to-ligand charge transfer state (MLCT) and a ligand field state (LF) on the photochemistry and photophysics of cobalamins.¹⁸ The MLCT and LF regions are characterized by changes in the relative contributions of corrin π and cobalt d orbitals. The MLCT state has a structure similar to the ground state structure, while in the LF state one or both of the axial bonds are elongated or dissociated. The location of the seam, the structure of the relaxed excited states, and the barriers for dissociation and internal conversion to the ground state depend on the chemical nature of the upper axial ligand and on the environment.

Given this basic structure, the photochemistry of cobalamins can be summarized by the pathways illustrated schematically in Figure 10. The relative importance of the different regions of the lowest singlet excited state is controlled by the details of the axial ligand and the environment. CNCbl undergoes rapid bond elongation to region I followed by internal conversion to the ground state on a picosecond time scale.^{17,32,42} The excited state is best characterized as a $\pi \rightarrow \sigma^*(d_z^2)$ ligand-to-metal charge transfer state (LMCT).^{39,40} The predicted pathway for de-excitation of CNCbl involves additional extension of the axial bonds reaching a seam with the GS (region IV).³³ The barrier for internal conversion is sensitive to the polarity of the solvent environment.³¹

Ethylcobalamin (EtCbl) and propylcobalamin (PrCbl) readily access the region II characterized by formation of a caged radical pair with unit quantum yield, although the pathway may also involve transient population of structures characterized by the MLCT state, X.^{30,43} AdoCbl also accesses region II followed by formation of a caged radical pair with unit quantum yield, although the pathway to this state is dependent

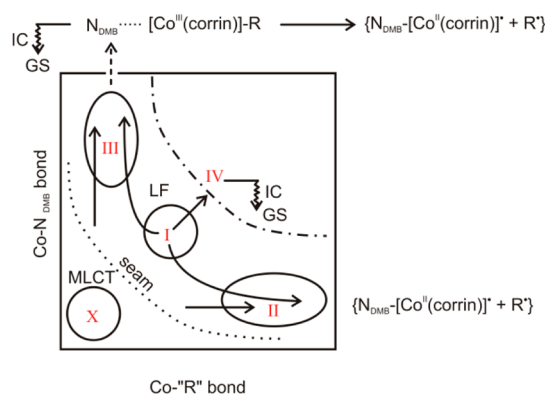


Figure 10. Schematic diagram of the significant regions and likely minima on the S₁ excited state surface of base-on cob(III)alamins. Potential outcomes of photoexcitation include homolysis of the Co–R bond, detachment of the N_{DMB} ligand, and internal conversion (IC) to the ground state (GS). The regions labeled X, I, II, III, and IV represent S₁ minima observed for different cob(III)alamins. The predicted pathway for de-excitation of CNCbl involves additional extension of the axial bonds reaching a seam with the GS. This cartoon is based on recent TD-DFT calculations.^{18,33,35–37}

on the environment,³¹ with transient population of a state characterized by elongation of the Co–N_{DMB} bond in water (region III),⁴⁴ elongation of both bonds (region I) in ethylene glycol,⁴⁴ and the MLCT state (region X) in glutamate mutase.^{45,46} MeCbl and HOCbl form an MLCT state having a structure similar to the ground state (region X) with internal conversion to the ground state dominating the decay of this state.^{35,47,48} Both of these compounds also exhibit wavelength dependent photochemistry with higher energy excitation accessing a channel that couples directly into the region II resulting in bond homolysis.

The transient absorption measurements on PhEtyCbl exhibit a weak broad absorption extending into the near IR and a blue-shifted $\alpha\beta$ -band (Figure 5c). The observed trends are consistent with elongation of the axial bonds and population of Co d_z² orbitals in a LMCT state similar to that observed for CNCbl. There is no evidence for dissociation of either axial ligand following excitation of PhEtyCbl. The absence of photoproduct formation under steady state illumination suggests that internal conversion to the ground state is complete. The sp hybridization of carbon bonded to cobalt has been proposed to lead to an inherently stronger Co–C- σ -bond and it also permits π -bonding interactions that further stabilize the bond against cleavage. The critical Co–C-bond of PhEtyCbl has, indeed, been shown to be remarkably short, suggested to be results of pi-bonding in the ground state.¹²

In arylcobalamins the sp² hybridization of the carbon bound to the cobalt center is also expected to stabilize the Co–C-bond, due to both, its sp²-character, as well as the possible π -bonding interactions with valence shell d-orbitals of cobalt. Interestingly, the “upper” aryl group of EtPhCbl and its ‘lower’ electron rich nucleotide base are oriented nearly parallel,¹¹ consistent with the possible relevance of extended pi-conjugation via the metal center. The much lower efficiency of photoinduced cleavage of the Co–C-bond of EtPhCbl (when compared to alkylcobalamins) suggests a stabilizing effect in the excited state, as well. The transient absorption measurements on EtPhCbl provide the first clear experimental evidence for photodissociation of the lower axial DMB ligand. The absorption spectrum of the excited state, with an $\alpha\beta$ -band

peaking at <450 nm, points to a LF minimum with an extended bond or dissociated lower axial ligand (region III). The presence of a strong excited state γ -band at 312 nm suggests that the upper axial ligand is also elongated. Base-off EtPhCbl does not possess a pronounced γ -band peak in this region while cob(II)alamin possess a strong γ -band at 312 nm. The excited state population branches between internal conversion to the ground state ($\sim 90\%$) and formation of a long-lived base-off EtPhCbl ($\sim 9\%$) on a 240 ps time scale. Bond homolysis is a minor pathway proceeding from the LF minimum, with a yield too small to be observed in the transient absorption measurements ($<1\%$). Unlike MeCbl and HOcbl, photohomolysis is independent of excitation wavelength and thus does not involve branching between electronic states during internal conversion to S_1 . The photochemical features of EtPhCbl are basically consistent with the photolysis pathway predicted by Kozłowski and co-workers for MeCbl following visible excitation.^{18,37}

CONCLUSIONS

The arylcobalamin EtPhCbl is decomposed by day light and it is classified as a light sensitive “antivitamin B₁₂”.¹¹ In contrast, the alkynylcobalamin PhEtyCbl is found photostable and, thus, it represents a “light insensitive potential antivitamin B₁₂”.¹² However, when observed here by femto- and picosecond transient absorption measurements, excitation of neither compound studied here results in significant dissociation of the Co–C-bond. Both of these potential “antivitamins B₁₂” form an excited state characterized by elongation of axial bonds, most notably the Co–N_{DMB}-bond. Photoexcited PhEtyCbl undergoes quantitative conversion to the ground state while EtPhCbl forms a long-lived base-off product, and undergoes Co–C-bond homolysis with $<1\%$ quantum yield. Thus, in contrast to previously studied organometallic cobalamins, such as AdoCbl and MeCbl (in both of which a saturated C atom is bound to cobalt), neither PhEtyCbl nor EtPhCbl (in which an unsaturated C atom is cobalt bound) provide efficient access to the “homolysis” channel following excitation in the visible or near-UV regions of the spectrum. Indeed, rapid complete deactivation of photoexcited alkynyl-cobalamins (such as PhEtyCbl) explains their striking inertness when exposed to day light. In contrast, the residual homolytic photoactivity of EtPhCbl (from access to the excited state bond homolysis channel) requires its protection from light when used as a reliable “antivitamin B₁₂” in long-term experiments with laboratory animals.¹¹ Absorption of daylight or sunlight turns this “antivitamin B₁₂” into a metabolically active vitamin B₁₂ form. Thus, EtPhCbl can be considered a photoresponsive “conditional antivitamin B₁₂”,⁸ in long-term experiments, as it exhibits a remarkably low quantum response. For the alternative application of “antivitamins B₁₂” as scaffolds for light-activated delivery of therapeutic agents with high spatiotemporal control cobalamins with considerably higher photolability than featured by EtPhCbl will be required. Suitable types of modification of the aryl-moiety appear to represent a useful design strategy in this direction. Work is currently underway to explore this hypothesis. Clearly, additional experimental and theoretical work is required to establish structural criteria for the design of such arylcobalamins that are highly photoactive and metabolically inert.

ASSOCIATED CONTENT

Supporting Information

The Supporting Information is available free of charge on the ACS Publications website at DOI: 10.1021/jacs.6b05299.

Steady state photolysis measurements on EtPhCbl and derivation of the equations for the description of species associated spectra assuming a sequential model (PDF)

AUTHOR INFORMATION

Corresponding Author

*rsension@umich.edu

Notes

The authors declare no competing financial interest.

ACKNOWLEDGMENTS

Support by the Austrian Science Fund (FWF, Project No. P-28892) and the U.S. National Science Foundation (CHE-1464584) is gratefully acknowledged.

REFERENCES

- (1) Banerjee, R.; Ragsdale, S. W. *Annu. Rev. Biochem.* **2003**, *72*, 209–247.
- (2) Kräutler, B.; Puffer, B. In *Handbook of Porphyrin Science*; Kadish, K. M., Smith, K. M., Guillard, R., Eds.; World Scientific: Singapore, 2012; Vol. 25, p 133–265.
- (3) Frey, P. A.; Hegeman, A. D. *Enzymatic Reaction Mechanisms*; Oxford University Press: New York, 2007.
- (4) Buckel, W.; Golding, B. T. *Annu. Rev. Microbiol.* **2006**, *60*, 27–49.
- (5) Banerjee, R. *Chemistry and Biochemistry of B12*; John Wiley and Sons: New York, 1999.
- (6) Scalabrino, G.; Peracchi, M. *Trends Mol. Med.* **2006**, *12*, 247–254.
- (7) Carmel, *Annu. Rev. Med.* **2000**, *51*, 357–375.
- (8) Kräutler, B. *Chem. - Eur. J.* **2015**, *21*, 11280–11287.
- (9) Gherasim, C.; Lofgren, M.; Banerjee, R. *J. Biol. Chem.* **2013**, *288*, 13186–13193.
- (10) Gruber, K.; Puffer, B.; Kräutler, B. *Chem. Soc. Rev.* **2011**, *40*, 4346–4363.
- (11) Ruetz, M.; Gherasim, C.; Gruber, K.; Fedosov, S.; Banerjee, R.; Kräutler, B. *Angew. Chem., Int. Ed.* **2013**, *52*, 2606–2610.
- (12) Ruetz, M.; Salchner, R.; Wurst, K.; Fedosov, S.; Kräutler, B. *Angew. Chem., Int. Ed.* **2013**, *52*, 11406–11409.
- (13) Chrominski, M.; Lewalska, A.; Karczewski, M.; Gryko, D. *J. Org. Chem.* **2014**, *79*, 7532–7542.
- (14) Chrominski, M.; Lewalska, A.; Gryko, D. *Chem. Commun. (Cambridge, U. K.)* **2013**, *49*, 11406–11408.
- (15) Mutti, E.; Ruetz, M.; Birn, H.; Kräutler, B.; Nexø, E. *PLoS One* **2013**, *8*, e75312.
- (16) Taylor, R. T.; Smucker, L.; Hanna, M. L.; Gill, J. *Arch. Biochem. Biophys.* **1973**, *156*, 521–533.
- (17) Rury, A. S.; Wiley, T. E.; Sension, R. J. *Acc. Chem. Res.* **2015**, *48*, 860–867.
- (18) Kozłowski, P. M.; Garabato, B. D.; Lodowski, P.; Jaworska, M. *Dalton Trans.* **2016**, *45*, 4457–4470.
- (19) Kutta, R. J.; Hardman, S. J. O.; Johannissen, L. O.; Bellina, B.; Messiha, H. L.; Ortiz-Guerrero, J. M.; Elias-Arnanz, M.; Padmanabhan, S.; Barran, P.; Scrutton, N. S.; Jones, A. R. *Nat. Commun.* **2015**, *6*, 7907.
- (20) Jost, M.; Simpson, J. H.; Drennan, C. L. *Biochemistry* **2015**, *54*, 3231–3234.
- (21) Jost, M.; Fernandez-Zapata, J.; Polanco, M. C.; Ortiz-Guerrero, J. M.; Chen, P. Y. T.; Kang, G.; Padmanabhan, S.; Elias-Arnanz, M.; Drennan, C. L. *Nature* **2015**, *526*, 536–U167.
- (22) Diez, A. I.; Ortiz-Guerrero, J. M.; Ortega, A.; Elias-Arnanz, M.; Padmanabhan, S.; de la Torre, J. G. *Eur. Biophys. J.* **2013**, *42*, 463–476.

- (23) Ortiz-Guerrero, J. M.; Polanco, M. C.; Murillo, F. J.; Padmanabhan, S.; Elias-Arnanz, M. *Proc. Natl. Acad. Sci. U. S. A.* **2011**, *108*, 7565–7570.
- (24) Shell, T. A.; Lawrence, D. S. *Acc. Chem. Res.* **2015**, *48*, 2866–2874.
- (25) Shell, T. A.; Shell, J. R.; Rodgers, Z. L.; Lawrence, D. S. *Angew. Chem., Int. Ed.* **2014**, *53*, 875–878.
- (26) Shell, T. A.; Lawrence, D. S. *J. Am. Chem. Soc.* **2011**, *133*, 2148–2150.
- (27) Snellenburg, J. J.; Laptinok, S.; Seger, R.; Mullen, K. M.; van Stokkum, I. H. M. *J. Stat. Software* **2012**, DOI: 10.18637/jss.v049.i03.
- (28) Spears, K. G.. Unpublished fast global fitting code that uses a variable projection algorithm for pump and repump experiments in Python language.
- (29) Pratt, J. M. *Inorganic Chemistry of Vitamin B₁₂*; Academic Press: New York, 1972.
- (30) Cole, A. G.; Yoder, L. M.; Shiang, J. J.; Anderson, N. A.; Walker, L. A., II; Banaszak Holl, M. M.; Sension, R. J. *J. Am. Chem. Soc.* **2002**, *124*, 434–441.
- (31) Harris, D. A.; Stickrath, A. B.; Carroll, E. C.; Sension, R. J. *J. Am. Chem. Soc.* **2007**, *129*, 7578–7585.
- (32) Shiang, J. J.; Cole, A. G.; Sension, R. J.; Hang, K.; Weng, Y.; Trommel, J. S.; Marzilli, L. G.; Lian, T. *J. Am. Chem. Soc.* **2006**, *128*, 801–808.
- (33) Lodowski, P.; Jaworska, M.; Andruniów, T.; Garabato, B. D.; Kozłowski, P. M. *Phys. Chem. Chem. Phys.* **2014**, *16*, 18675–18679.
- (34) Gruber, K.; Krautler, B. *Angew. Chem., Int. Ed.* **2016**, *55*, 5638–5640.
- (35) Wiley, T. E.; Miller, W. R.; Miller, N. A.; Sension, R. J.; Lodowski, P.; Jaworska, M.; Kozłowski, P. M. *J. Phys. Chem. Lett.* **2016**, *7*, 143–147.
- (36) Lodowski, P.; Jaworska, M.; Garabato, B. D.; Kozłowski, P. M. *J. Phys. Chem. A* **2015**, *119*, 3913–3928.
- (37) Lodowski, P.; Jaworska, M.; Andruniów, T.; Garabato, B. D.; Kozłowski, P. M. *J. Phys. Chem. A* **2014**, *118*, 11718–11734.
- (38) Kornobis, K.; Kumar, N.; Lodowski, P.; Jaworska, M.; Piecuch, P.; Lutz, J. J.; Wong, B. M.; Kozłowski, P. M. *J. Comput. Chem.* **2013**, *34*, 987–1004.
- (39) Solheim, H.; Kornobis, K.; Ruud, K.; Kozłowski, P. M. *J. Phys. Chem. B* **2011**, *115*, 737–748.
- (40) Lodowski, P.; Jaworska, M.; Kornobis, K.; Andruniów, T.; Kozłowski, P. M. *J. Phys. Chem. B* **2011**, *115*, 13304–13319.
- (41) Lodowski, P.; Jaworska, M.; Andruniów, T.; Kumar, M.; Kozłowski, P. M. *J. Phys. Chem. B* **2009**, *113*, 6898–6909.
- (42) Wiley, T. E.; Arruda, B. C.; Miller, N. A.; Lenard, M.; Sension, R. J. *Chin. Chem. Lett.* **2015**, *26*, 439–443.
- (43) Sension, R. J.; Harris, D. A.; Cole, A. G. *J. Phys. Chem. B* **2005**, *109*, 21954–21962.
- (44) Yoder, L. M.; Cole, A. G.; Walker, L. A., II; Sension, R. J. *J. Phys. Chem. B* **2001**, *105*, 12180–12188.
- (45) Sension, R. J.; Harris, D. A.; Stickrath, A.; Cole, A. G.; Fox, C. C.; Marsh, E. N. G. *J. Phys. Chem. B* **2005**, *109*, 18146–18152.
- (46) Sension, R. J.; Cole, A. G.; Harris, A. D.; Fox, C. C.; Woodbury, N. W.; Lin, S.; Marsh, E. N. G. *J. Am. Chem. Soc.* **2004**, *126*, 1598–1599.
- (47) Shiang, J. J.; Walker, L. A., II; Anderson, N. A.; Cole, A. G.; Sension, R. J. *J. Phys. Chem. B* **1999**, *103*, 10532–10539.
- (48) Walker, L. A., II; Jarrett, J. T.; Anderson, N. A.; Pullen, S. H.; Matthews, R. G.; Sension, R. J. *J. Am. Chem. Soc.* **1998**, *120*, 3597–3603.